

FAST CIGS CO-EVAPORATION PROCESSES BY CONTROLLED RAPID RAMPING OF THERMAL EVAPORATION SOURCES TO VERY HIGH RATES

Alexander Marienfeld, Christopher Eisele, Heiko Schuler
Dr. Eberl MBE-Komponenten GmbH, Josef-Beyerle-Straße 18/1, D71263 Weil der Stadt

ABSTRACT: Fast CIGSe co-evaporation processes with steep Ga-grading require highly dynamic thermal evaporation sources with deposition rates up to several nm/s. In this work we demonstrate the feasibility of fast ramping rates for copper evaporation from a standard PEZ-W 63-160 effusion cell. This source type is widely used in CIGSe research systems and pilot lines. Originally, the PEZ-W 63-160 was designed for a constant rate operation and very little is known for dynamic operation. Deposition rates up to 120nm/min are demonstrated for a typical substrate distance with ramping times of less than 5min from idle temperature to more than 1400°C. The built-in thermocouple provides a good monitor even to highly dynamic evaporation rates. As a consequence, standard deposition systems can be upgraded for the development of fast processes and the transfer to inline production systems becomes much easier.

Keywords: CIGS, Co-evaporation, Physical Vapor Deposition, thermal evaporation, effusion cell

1 INTRODUCTION

In recent years, the need for highly productive photovoltaic production tools to lower the cost has increased dramatically. Even though CIGSe is one of the most promising cell technologies, with laboratory efficiencies up to 20.4% [1-3], the commercial production of CIGSe-modules on the multi-megawatt scale remains a challenge. A key issue to reach a higher productivity is a strongly increased throughput and uptime of the absorber formation equipment. In case of the co-evaporation processes this leads to evaporation sources with larger capacities, higher evaporation rates and better material utilization configured for wider deposition windows. Today the thermal evaporation sources are not the limiting factor for higher throughput. Our current evaporation source technology is at least one tool generation ahead of the deposition rate requirements of state-of-the-art production tools. The crucial question is, whether the absorber formation process is fast enough to realize compact production tools with a short process time and whether a fast process can be transferred to such a tool.

The formation speed can be investigated on small area samples [4,5]. Molecular beam epitaxy (MBE) like co-evaporation systems usually work with moderate evaporation rates below 10 nm/min. Typically the rate of the evaporation source is calibrated and kept constant over the complete deposition run. Mechanical shutters are used to switch the beam flux.

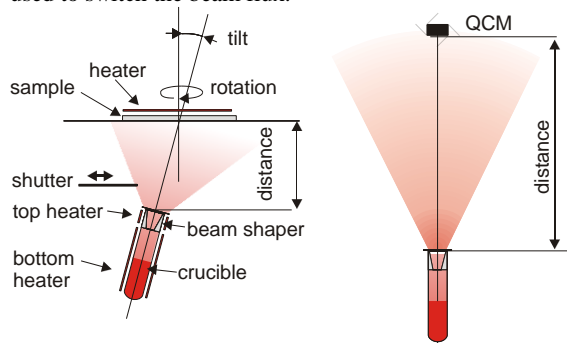


Figure 1: Typical deposition arrangement of a MBE-like system (left). Test setup to characterize the thermal evaporation sources (right).

Fig. 1 (left) shows a typical deposition arrangement of a MBE-like deposition system. The sample is mounted

face-down in a rotating heated sample holder (manipulator). The thermal evaporation sources (effusion cells) are arranged below the sample holder. Typically they are equipped with round crucibles and the orifice is directed onto a rotating substrate. The tilt of the source, the displacement, the distance and the shape of the vapor plume results in a flux distribution on the substrate. To achieve a good homogeneity the substrate is rotated continuously during the deposition. The homogeneity increases with increasing substrate-source distance. On the other hand the deposition rate on the substrate is reduced inversely with the square of the distance. MBE-Komponenten uses sophisticated proprietary deposition simulation software to design the deposition arrangement and predict the homogeneity very precisely (better 1%). The deposition rate cannot stay at high level in a MBE-like system because too much material would be deposited on the shutter and the filling capacity would reduce the deposition runs dramatically. Therefore a shorter process time with higher rates require a highly dynamic and reproducible operation of the thermal evaporation sources. Rates of more than 100 nm/min on the substrate are required to reach copper deposition times below 2min for standard CIGSe absorber of about 2µm thickness.

In order to investigate the limits, the PEZ-W 63-150 was tested in dynamic operation mode and high evaporation rates.

2 EXPERIMENT

In the experiment the deposition rate has been determined by a water-cooled quartz crystal monitor (QCM) located in cell axis at a defined distance to the source orifice (Figure 1 right). The source was loaded with high purity copper (316,5g). The crucible is equipped with a beam shaper to form the vapor plume and direct the vapor towards the substrate. Additionally the effect of the filling level on the vapor plume is strongly reduced. The PEZ-W 63-160 is a dual filament source with a top heater for the beam shaper and a bottom heater for the melt (Figure 1 left). The top heater keeps the beam shaper hot enough to prevent condensation and the bottom heater is used to adjust the evaporation rate. A thermocouple is applied to measure the temperature of the melt close to the crucible. A series of different power ramps were applied to the bottom heater, while the top heater was set to different constant values. First the evaporation source was ramped up and down slowly followed by faster

cycles to emphasize on the different evaporation characteristics.

3 THEORY

The evaporation rate is proportional to the vapor pressure. It is difficult to measure the exact temperature of the melt, but the evaporation rate can be measured directly or determined for example by the weight loss. Here the relation between the evaporation rate and the temperature of the melt in the effusion cell is derived. The vapor pressure of Cu can be fitted using equation 1 with the parameters A and B. (for other materials see Reference 6)

$$p_s(T) = 10^{A - B/T[K]} = 10^{9.284 - 17073/T[K]} \text{ [mbar]} \quad (1)$$

The evaporation rate $j(T)$ can be recalculated from the melt temperature (T) using equation 2:

$$j(T) = w \cdot \frac{p_s(T) \cdot c(T)}{4 \cdot k \cdot T} \text{ [atoms/(m}^2 \text{ sec)]} \quad (2)$$

w: probability (=1 for a free evaporation, <1 for a backpressure)

$p_s(T)$: vapor pressure [Pa]

$c(T)$: thermal velocity $c = \sqrt{\frac{8 \cdot R \cdot T}{\pi \cdot M}}$

M: Molar mass [kg/mol]

In a thermal evaporation source with a beam shaping insert a certain backpressure is established. In a simple model the probability w can be derived from the orifice area and the surface area of the melt.

In conclusion the source evaporation rate $r_{\text{source}}(T)$ for the molecular regime can be determined using equation 3:

$$r_{\text{source}}(T) = \frac{j(T)}{N_A} \cdot M \cdot A \cdot Tr \quad (3)$$

N_A : Avogadro constant

A: beam shaper entry area

Tr: beam shaper transmission

The beam shaper transmission is calculated using a Monte-Carlo simulation. Here the trajectory of a huge number of evaporated atoms is analyzed. Similarly the rate distribution at the substrate or the QCM plane can be calculated. As the Monte Carlo simulation is very precise only one measured point in the plume is needed to recalculate the total evaporation rate of the source. The ratio between the rate at a defined small area and the integral rate of the source we call the geometrical factor for this small area (typically 1 cm²). The accuracy of this method is demonstrated later by comparing the weight loss in the source with the totally evaporated copper calculated from the thickness of the layer at the QCM.

4 RESULTS

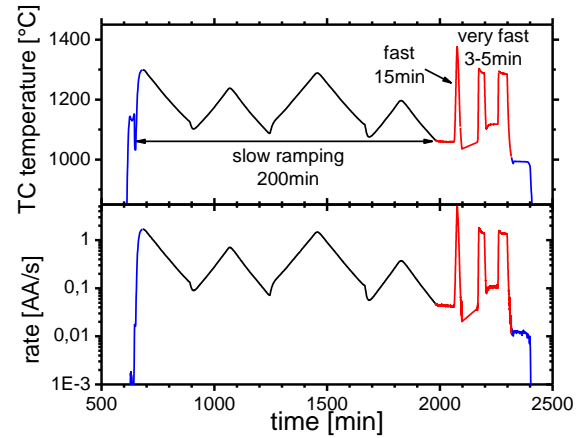


Figure 2: Ramping sequence of the effusion cell. Top: temperatures as measured by a thermocouple close to the crucible; bottom: corresponding rate as measured by the QCM

The ramping sequence of the source can be depicted from Figure 2. In the top diagram the temperature measured by the thermocouple is plotted, in the bottom diagram the rate determined by the QCM is shown. The different colors indicate the experimental values for initial melting of the copper and freezing of the melt (blue), the slow operation mode data (black) and the dynamic mode data (red).

During initial ramp-up moderate top and bottom heater settings had been used until the target temperatures were reached. In the slow operation mode a current ramp of about 200min length was applied to the bottom heater for demonstration of evaporation characteristics under stabilized conditions.

The experimental results are shown in Figure 3. The plotted evaporation rate is measured at the quartz crystal monitor in a comparably large distance to the source compared to the theoretical predicted rate derived from section 3. For better comparability of the data the rate equivalent for typical MBE-system has been calculated. The rate shown on the right axis corresponds to a source to substrate spacing of about 350mm and the substrate is in perpendicular orientation towards the source axis.

The data presented in Figure 3 is in good agreement with theory. At low temperatures the rate deviates about 20% from theoretical predicted values. The rate difference can be attributed to the influence of the top heater. The surface temperature of the melt will deviate from the TC-temperature reading due the comparably high top heater input.

After several slow ramps, with 3 different top-heater settings, the dynamic mode experiment was conducted. While the top heater was set to a fixed value, three aggressive ramps have been applied to the bottom heater with temperature ramp-up times of 15, 5 and 3 minutes respectively.

In the first cycle the current was ramped up in 600s directly followed by a ramp-down within 780s. In the second and third cycle the current was ramped-up during 60s, the power was kept for 130s respectively 90s and then ramped down in 30s to a constant high rate level at which the source was stabilized. The stabilization was followed by a fast ramp down.

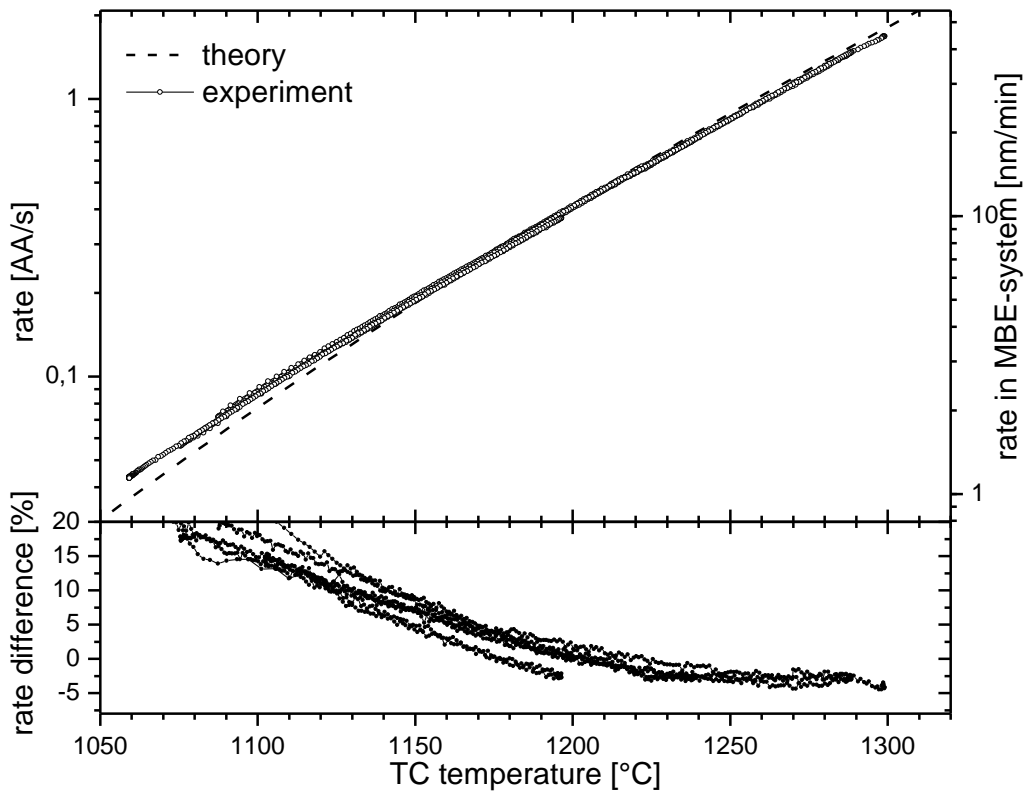


Figure 3: Experimental results for three cycles in slow operation mode. Top: Copper evaporation rates obtained by QCM measurement (symbols) theoretical predicted rate (dashed line); bottom: deviation of the measured rate from the predicted theoretical rate.

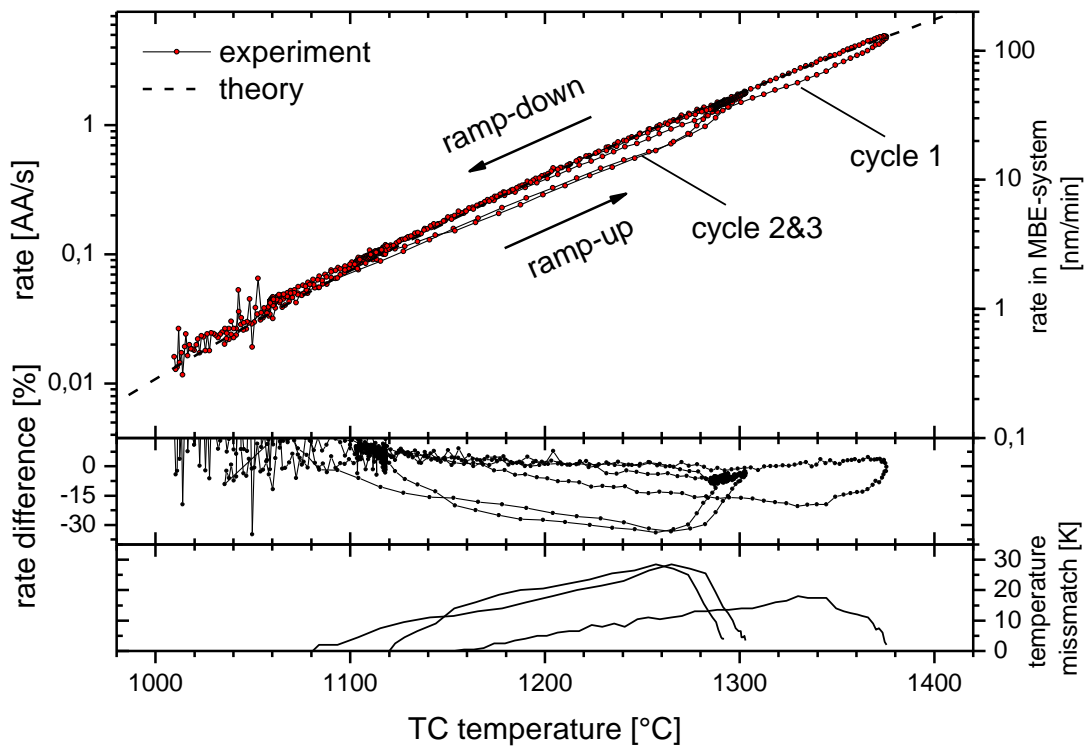


Figure 4: Experimental results for dynamic operation mode. Top: Copper evaporation rate obtained by QCM measurement (symbols) theoretical predicted rate (dashed line); middle: deviation of the measured rate from the predicted theoretical rate; bottom: temperature mismatch of measured rate to predicted rate during ramp-up.

The results are shown in Figure 4. When ramping up the measured evaporation rate deviates from the theoretical rate values for the corresponding TC-temperature. This divergence clearly indicates the impact of the heater on the TC-temperature reading. For the fast cycle the difference of the rate goes up to 20% which corresponds to a temperature mismatch of about 18K. Both very fast cycles give a rate difference of about 34% equivalent to roughly 28K temperature mismatch. The cumulated rate offset sums up to a deficiency in the deposited film in a MBE system of about 44nm for the fast cycle and 16nm for the very fast cycles. The total theoretical deposited rate is 410nm and 120nm respectively. The progression of cycle 2 and 3 are very similar showing a good reproducibility of the evaporation characteristic.

In case of fast ramp-down the measured rate follows theory remarkably well. The 1/e decay rate is in the order of 2min; bottom heaters were ramped down fast and the top heater was kept constant. Note that a larger copper load will lead to a slower ramp down.

It is worth to emphasize, that no fitting parameters have been applied to the model used to determine the evaporation characteristic. Theoretical values are purely derived from experimental data or values derived by geometrical considerations. E.g. the temperature offset of the thermocouple to the surface temperature of the copper melt has been determined at melting level.

To analyze the validity of the model, we compared the mass loss of the copper ingot by three independent ways. First we measured the mass loss before and after the process (30,5g). Secondly we determined the amount of evaporated material by integrating the rate measured at the QCM. When applying the geometrical factor and distance this results in a value of 30.2g. Thereby accurateness of the geometrical factor (see section 3) applied to determine the shape of the evaporation plume is within 1%. Thirdly we used the evaporation model and evaluated the surface temperature of the melt from the TC reading. The integration of the source evaporation rate determined from equation (3) gives a value of 30.5g. This indicates that the accumulated error in the deposition time of over 30h at different temperature levels is quite low and the assumptions made in the model are valid. In conclusion we found an overall excellent consistency of all approaches circumstantiating the model for the evaporation characteristic.

4 CONCLUSIONS AND OUTLOOK

We have shown that the rate is highly predictable by TC reading and evaporation characteristic of the source is well understood. This is the prerequisite for higher dynamic ramping of the source. Fast ramp-up of the source leads to a mismatch of the actual rate and the theoretical predicted rate derived from the thermocouple. However this rate discrepancy seems to be reproducible. Thus precise dynamic ramping of the source is applicable for a calibrated evaporation characteristic. With a precise dynamic ramping, the rate profiles of inline deposition systems can be reproduced. Process development and transfer from MBE-like co-evaporation systems to inline production systems become much easier.

5 REFERENCES

- [1] A. Chirilă; , S. Bücheler , F. Pianezzi , P. Bloesch , C. Gretener and A. R. Uhl "Highly efficient Cu(In,Ga)Se₂ solar cells grown on flexible polymer films", *Nat. Mater.*, vol. 10, pp.857-861 2011
- [2] Jackson, P., Hariskos, D., Lotter, E., Paetel, S., Wuerz, R., Menner, R., Wischmann, W. and Powalla, M. (2011), "New world record efficiency for Cu(In,Ga)Se₂ thin-film solar cells beyond 20%". *Prog. Photovolt: Res. Appl.*, 19: 894–897. doi: 10.1002/pip.1078
- [3] Repins, I., Contreras, M. A., Egaas, B., DeHart, C., Scharf, J., Perkins, C. L., To, B. and Noufi, R. (2008), "19.9%-efficient ZnO/CdS/CuInGaSe₂ solar cell with 81.2% fill factor". *Prog. Photovolt: Res. Appl.*, 16: 235–239. doi: 10.1002/pip.822
- [4] Chirilă, A., Seyrling, S., Buecheler, S., Guettler, D., Nishiwaki, S., Romanyuk, Y. E., Bilger, G. and Tiwari, A. N. (2012), "Influence of high growth rates on evaporated Cu(In,Ga)Se₂ layers and solar cells". *Prog. Photovolt: Res. Appl.*, 20: 209–216. doi: 10.1002/pip.1122
- [5] O. Lundberg, M. Bodegård, L. Stolt "Rapid growth of thin Cu(In,Ga)Se₂ layers for solar cells" *Thin Solid Films*, Vol. 431–432, 1 May 2003, Pages 26-30, [http://dx.doi.org/10.1016/S0040-6090\(03\)00241-4](http://dx.doi.org/10.1016/S0040-6090(03)00241-4).
- [6] <http://www.mbe-komponenten.de/selection-guide/element.php>